JOURNAL OF SOLID STATE CHEMISTRY 51, 364–375 (1984)

Temperature Dependence of the Structure and Bonding in Deuterated Cu(II) Tutton's Salt

B. J. HATHAWAY

Chemistry Department, University College, Cork, Ireland

AND A. W. HEWAT[1]

Institut Max von Laue-Paul Langevin BP 156X, 38042 Grenoble Cedex, France

Received June 20, 1983; in revised form October 5, 1983

The detailed structure of deuterated Cu(II) Tutton's salt, $Cu(OD_2)_6(ND_4)_2(SO_4)_2$, has been determined at 5, 50, 123, 150, 203, 250, and 295 K by neutron powder diffraction. Near absolute zero, Cu(II) is at the center of a tetragonally elongated oxygen octahedron formed by the water molecules, but Cu—O(8) is elongated as in the alkali isomorphs, rather than Cu—O(7) as in the hydrogenous ammonium salt. At higher temperatures, the $P2_1/a$ unit cell is stretched along c, with a phase transition predicted near 340 K due to hindered rotation of the $(ND_4)^+$ ions. The CuO_6 octahedron is then subjected to a rhombic distortion, which may finally result in a tetragonally compressed octahedron above this transition temperature. Such transitions from elongated to compressed tetragonal Cu(II) coordination are usually interpreted as order–disorder of the Jahn–Teller elongated Cu(II)—O axis, rather than changing packing requirements for the remainder of the structure. This work emphasizes the importance of the hydrogen bonds in determining the structure.

Introduction

The structural chemistry of cupric compounds is a "subject of outstanding interest" (*1*). To a first approximation, Cu(II) usually prefers to form four coplanar bonds, with one or two additional weaker bonds out of the plane. It can then occupy the center of an elongated octahedra of N, O, F, or Cl atoms. In some cases, such as $Cu(dien)_2(NO_3)_2$, the octahedra are compressed rather than elongated, with two shorter and four longer bonds (*2*). In others, such as Cu(II) Tutton's salt $Cu(OH_2)_6(NH_4)_2(SO_4)_2$, a temperature-dependent rhombic distortion of the $Cu(OH_2)_6^{2+}$ groups is observed (*3*): at room temperature the octahedra are compressed, but at low temperature they apparently approach the expected elongated configuration. Such octahedral coordination is then of special interest because of these so-called Jahn–Teller distortions.

Both compressed octahedral coordination, and temperature-dependent rhombic distortions, can be explained in terms of the usual elongated octahedral coordination if it is supposed that the axis of elongation fluctuates at high temperatures between at least two of the three possible orthogonal directions—fluxional behavior (*4*).

[1] To whom correspondence should be addressed.

0022-4596/84 $3.00

In some complexes there is necessarily an unsymmetrical octahedral coordination for Cu(II), simply because of stresses produced by the dimensions of the remaining structural units. We had hoped that in a relatively simple structure such as Cu(II) Tutton's salt (monoclinic $P2_1/a$, 700-Å^3 cell), the Cu(II) coordination would be largely determined by Cu(II)—O bonding rather than by the packing requirements of the remainder of the structure.

Essentially $Cu(OH_2)_6(NH_4)_2(SO_4)_2$ consists of hexahydrated ions $Cu(OH_2)_6^{2+}$ which are hydrogen (and electrostatically) bonded to SO_4^{2-} groups. The remaining $(NH_4)^+$ ions are also hydrogen bonded to the sulfate oxygens, since the water oxygens forming the distorted CuO_6 octahedron are largely isolated from other atoms. Recent X-ray measurements (*3, 5*) have shown that the strong rhombic distortion observed at room temperature is reduced at 123 K. It is of interest to extend these measurements to near absolute zero to see if the distortion disappears entirely in the lowest energy state of the lattice, and to plot the distortion at many more temperature points to understand its origin. Neutron powder diffraction was chosen as a rapid method of measuring the structure at many different temperatures down to absolute zero, and at the same time obtaining better information about the hydrogen bonding than is possible with X rays. As we shall see, this is of particular interest in the case of the $(NH_4)^+$ ions. It does require the use of deuterated samples, but it is of interest in itself to compare the hydrogenous and deuterated salts.

Experiment

Deuterated Tutton's salt was prepared by dissolving the hydrogenous material in the minimum quantity of hot D_2O, boiling to concentrate, adding more D_2O, and repeating this cycle five or six times. The final product was dried with P_2O_5 in a vacuum dessicator and recrystallized from pure D_2O. In this way it was estimated that at least 98% of the hydrogen atoms had been replaced by deuterium. This was confirmed by the neutron diffraction experiment, which showed negligible sample absorption, low background scattering, and in the refinement of the data, a scattering length appropriate for pure deuterium. Both absorption and background are high in the presence of hydrogen, and much longer counting times would have been necessary for a hydrogenous powder sample.

A 16-mm-diameter vanadium sample can was tightly packed to a depth of 20 mm with the deuterated Tutton's salt, and sealed to prevent reexchange with atmospheric water. Cadmium foils helped locate the sample in the neutron beam and eliminate scattering from other materials. In fact, the experimental geometry and shielding ensured that no extra diffraction lines, either from the sample can or from the cryostat, could enter the counters. The cryostat was of the standard ILL helium flow type for which the temperature could be controlled by the instrument computer to ±2° within the range 1.5 to 310 K.

At each temperature, the high resolution neutron powder diffractometer D1A (*6*) was scanned over the 2θ angular range 6 to 158° at 0.05° steps, for a total time of 11 hr. Up to 30 min was allowed between runs for the computer to change the temperature, which in a first experiment was chosen as 5, 123, 203, and 295 K to coincide with the earlier X-ray measurements. In a second experiment some days later, the structure was determined at the additional temperatures 50, 150, and 250 K, each run again lasting about 11 hr. The results from each of the 10 counters were automatically corrected for relative efficiencies and angular displacements, and summed to produce a single profile covering the entire angular range for each temperature (Fig. 1).

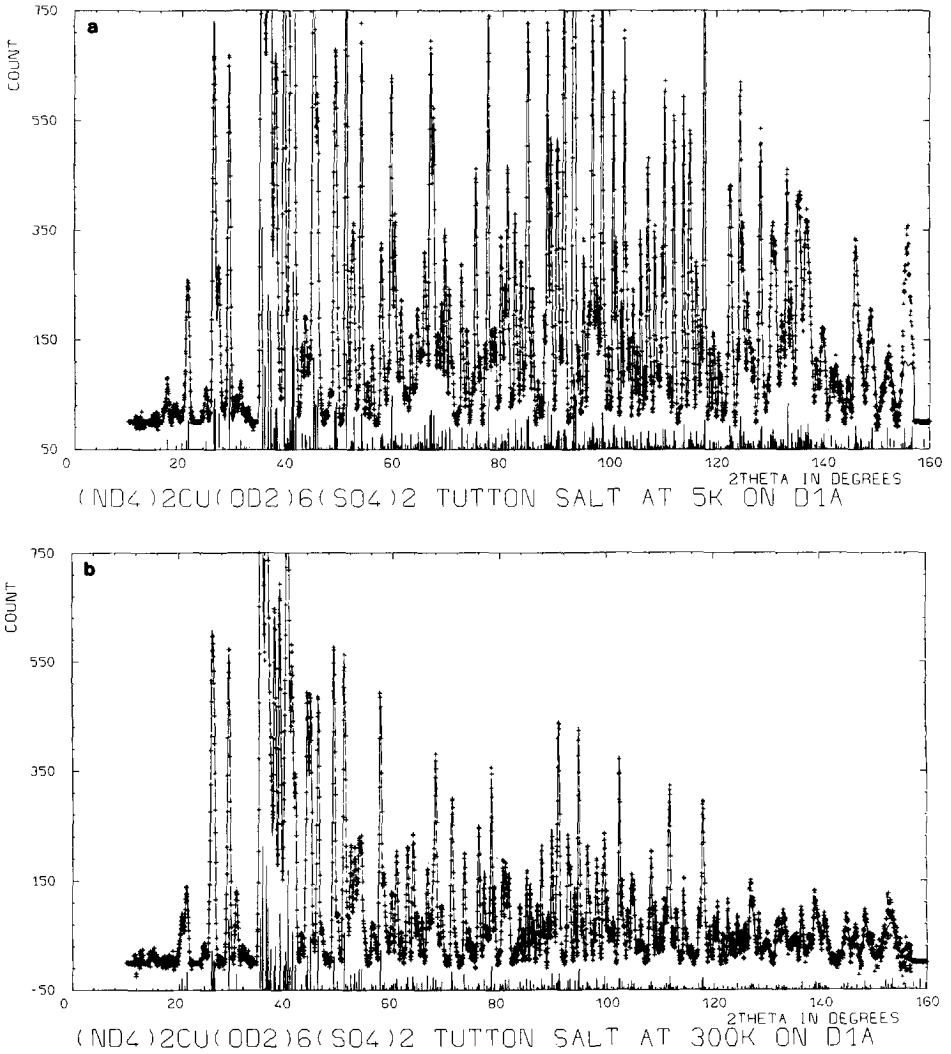

FIG. 1. Observed and calculated neutron powder diffraction patterns at (a) 5 K and (b) 300 K. The bars along the 2θ axis represent the positions and strengths of the contributing reflexions.

Calculations

All data and results were collated and examined using the POWDER program (*7*) on the ILL DEC-KL10 computer system. A modified Rietveld program (*8, 9*) was used to refine the profiles at each temperature after subtracting a background measured at 2θ points throughout the range. Two models were used, based on the earlier room temperature X-ray and neutron measurements of the hydrogenous salt (*10, 11*). In the first, isotropic temperature factors were refined for each type of atom (there are two types of deuterium—on water molecules and on ammonium ions). This model, with 62 structural parameters plus 10 others, gave good agreement with the experimental profile, especially at low temperatures: at higher temperatures, it was evi-

TABLE I

LATTICE DIMENSIONS a, b, c (Å) AND ANGLE β FOR D-Cu(II) TUTTON'S SALT

	Temperature (K)						
	5	50	123	150	203	250	295
a	9.4080(1)	9.4065(1)	9.4066(1)	9.4041(1)	9.3986(1)	9.3723(1)	9.3089(1)
b	12.6849(1)	12.6845(2)	12.6892(1)	12.6859(2)	12.6748(2)	12.6274(2)	12.5286(2)
c	6.0707(1)	6.0716(1)	6.0815(1)	6.0874(1)	6.1045(1)	6.1365(1)	6.2032(1)
β	107.152 (1)	107.151 (1)	107.128 (1)	107.100 (1)	107.004 (1)	106.769 (1)	106.391 (1)
V	692.25 (2)	692.24 (2)	693.71 (2)	694.12 (2)	695.41 (2)	695.36 (2)	694.06 (2)
R_p	6.4	6.9	5.3	6.7	6.3	6.4	8.2
R_I	4.3	4.4	3.1	4.1	4.6	3.7	5.4

Note. R_p is the R-factor for the complete diffraction profile, and R_I that for the integrated line intensities: the R-factor R_F usually quoted by crystallographers, is about half of R_I. All numbers in parentheses here and elsewhere are statistical standard deviations in the last digits quoted for the preceding value. Systematic errors in the neutron wavelength (±0.001 Å) or temperature (±2 K) are not included.

dent that large deuterium B-factors indicated strong libration of the ammonium ions. In the second model, all deuterium atoms were permitted to vibrate anisotropically and independently, requiring a total of 132 parameters. At room temperature, the strong libration of the ammonium ion, and to a lesser extent the water molecules, is obvious in the ORTEP plot. The fit to the higher temperature data in particular, was then considerably improved, especially at high angles. For example, at 295 K, R-profile fell from 11.5% with isotropic B-factors to 8.2% with anisotropic deuterium vibration. The R-factor R_I for integrated line intensities, which is approximately twice the conventional crystallographic R-factor, was now about 4% for all temperatures (Table I) compared to 9% for isotropic deuterium B's at 295 K (the scattering length of deuterium is large for neutrons). The agreement between the observed and calculated diffraction patterns (Fig. 1) is good at all temperatures, even though the profiles change considerably due to changes in the lattice constants (Fig. 2). All quoted results then refer to the second model with anisotropic deuterium vibration.

It is satisfying to see that the thermal ellipsoid axes do correspond quite well with the N—D and O—D bond directions, with

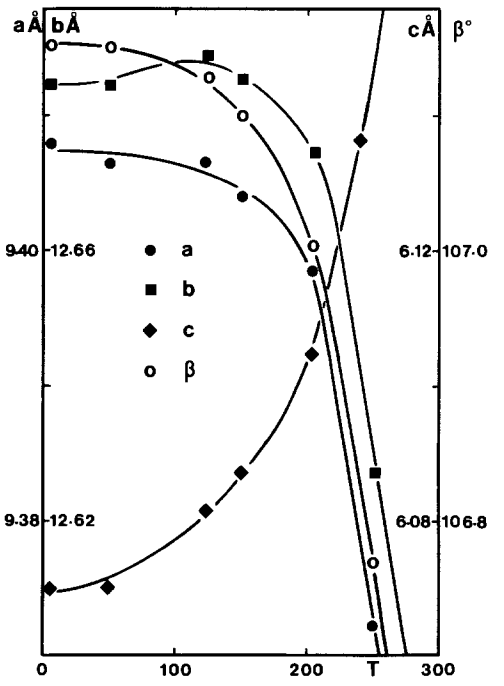

FIG. 2. The lattice dimensions and angle in Cu(II) Tutton's salt change remarkably with temperature. The c axis expands with the approach of the ND_4 flipping transition predicted near 340 K, with corresponding contraction of the a and b dimensions.

TABLE II

ATOMIC COORDINATES x, y, z, MULTIPLIED BY 10,000, AND AVERAGE ISOTROPIC VIBRATION PARAMETERS B_{av}

Atoms	x	y	z	B_{av}	Atoms	x	y	z	B_{av}
Cu(1)	0	0	0	0.13	O(8)	−1802(5)	1123(4)	508(7)	0.08
	0	0	0	0.38		−1810(6)	1117(5)	503(8)	0.38
	0	0	0	0.40		−1826(5)	1128(4)	472(6)	0.39
	0	0	0	0.72		−1830(6)	1125(5)	471(8)	0.99
	0	0	0	0.56		−1826(6)	1136(4)	486(8)	0.94
	0	0	0	1.15		−1810(6)	1131(4)	472(8)	1.48
	0	0	0	1.17		−1760(8)	1134(6)	441(10)	2.25
S(2)	3853(8)	1452(6)	7486(13)	0.10	O(9)	102(5)	−655(4)	2950(7)	0.08
	3866(8)	1457(6)	7539(13)	0.21		102(5)	−659(4)	2942(7)	0.38
	3841(7)	1457(5)	7510(11)	0.43		68(5)	−650(3)	2936(6)	0.39
	3881(8)	1441(6)	7525(12)	0.56		88(6)	−647(4)	2932(7)	0.99
	3874(8)	1442(6)	7543(11)	0.70		80(5)	−649(4)	2931(7)	0.94
	3912(9)	1443(6)	7449(12)	1.04		52(6)	−633(4)	2905(7)	1.48
	3955(11)	1417(8)	7477(17)	1.19		14(8)	−639(5)	2831(10)	2.25
O(3)	3805(5)	2382(3)	6056(7)	0.12	N(10)	1252(4)	3646(3)	3770(6)	0.07
	3813(5)	2389(3)	6048(7)	0.31		1246(5)	3653(3)	3775(6)	0.09
	3802(4)	2391(3)	6066(6)	0.42		1228(4)	3644(2)	3769(5)	0.28
	3808(5)	2389(3)	6060(6)	0.90		1244(5)	3647(3)	3763(7)	1.00
	3830(4)	2391(3)	6056(6)	0.73		1244(4)	3618(3)	3720(7)	1.07
	3870(4)	2375(3)	6064(7)	1.87		1230(4)	3609(4)	3717(8)	1.62
	3983(6)	2372(5)	6097(10)	2.80		1263(6)	3542(5)	3704(9)	2.68
O(4)	5260(4)	879(3)	7758(6)	0.12	D(11)	436(5)	3474(3)	2308(7)	0.58
	5281(5)	880(3)	7742(7)	0.31		446(5)	3464(3)	2320(8)	0.82
	5270(4)	888(3)	7740(6)	0.42		444(4)	3463(3)	2333(6)	0.76
	5278(4)	879(3)	7747(7)	0.90		455(5)	3456(4)	2338(8)	1.29
	5281(4)	872(3)	7741(6)	0.73		445(5)	3450(3)	2268(8)	1.29
	5301(5)	851(3)	7733(7)	1.87		509(5)	3431(4)	2307(8)	1.77
	5358(6)	836(4)	7777(10)	2.80		532(7)	3408(5)	2242(10)	2.60
O(5)	2601(4)	727(3)	6278(7)	0.12	D(12)	2042(5)	3040(3)	4203(8)	0.99
	2591(5)	733(3)	6280(7)	0.31		2036(5)	3056(4)	4203(8)	0.99
	2621(4)	729(3)	6278(6)	0.42		2030(4)	3069(3)	4180(7)	1.04
	2600(5)	735(3)	6282(7)	0.90		2038(5)	3049(3)	4175(8)	1.50
	2609(4)	725(3)	6276(7)	0.73		2040(5)	3072(3)	4165(8)	1.47
	2618(5)	733(3)	6286(7)	1.87		2025(6)	3062(4)	4086(9)	2.41
	2683(6)	731(5)	6238(9)	2.80		2045(9)	3035(6)	3928(14)	3.85
O(6)	3750(5)	1716(3)	9798(7)	0.12	D(13)	844(4)	3768(3)	5131(7)	0.61
	3744(5)	1730(3)	9805(8)	0.31		835(5)	3776(3)	5138(7)	0.71
	3741(4)	1728(3)	9793(6)	0.42		846(4)	3755(3)	5147(6)	0.79
	3733(5)	1718(3)	9783(7)	0.90		841(5)	3747(4)	5140(8)	1.48
	3713(4)	1728(3)	9722(7)	0.73		835(5)	3738(4)	5112(8)	1.54
	3736(5)	1741(3)	9671(7)	1.87		820(5)	3680(5)	4980(10)	2.88
	3753(7)	1731(5)	9643(10)	2.80		777(8)	3545(8)	4910(12)	4.69
O(7)	1506(5)	1083(3)	1625(8)	0.08	D(14)	1776(4)	4314(4)	3499(7)	0.90
	1507(6)	1070(3)	1604(9)	0.38		1768(5)	4322(4)	3498(8)	0.96
	1512(5)	1071(3)	1630(8)	0.39		1753(4)	4316(3)	3506(6)	0.98
	1504(5)	1078(4)	1635(9)	0.99		1765(5)	4323(4)	3502(8)	1.33
	1535(5)	1081(3)	1611(9)	0.94		1728(5)	4303(4)	3499(8)	1.52
	1531(5)	1102(4)	1668(9)	1.48		1726(5)	4287(4)	3519(9)	2.13
	1595(7)	1109(5)	1654(11)	2.25		1689(8)	4224(7)	3521(13)	3.88

TABLE II—*Continued*

Atoms	x	y	z	B_{av}	Atoms	x	y	z	B_{av}
D(15)	1954(4)	929(3)	3266(7)	0.65	D(18)	−1576(4)	1853(3)	261(7)	0.78
	1957(5)	932(3)	3264(7)	0.78		−1581(4)	1862(4)	277(7)	0.80
	1961(4)	939(2)	3282(6)	0.74		−1582(4)	1852(3)	270(7)	1.06
	1966(4)	929(3)	3276(7)	0.96		−1579(4)	1863(3)	275(7)	1.18
	1969(4)	944(3)	3288(7)	0.93		−1578(4)	1853(4)	254(7)	1.12
	2012(5)	927(3)	3257(6)	1.39		−1584(4)	1857(3)	184(8)	1.77
	2070(6)	925(4)	3226(8)	1.77		−1560(5)	1858(5)	85(11)	2.24
D(16)	2331(4)	1249(3)	994(7)	0.60	D(19)	−850(4)	−606(3)	3340(6)	0.51
	2333(4)	1249(3)	998(7)	0.74		−842(5)	−617(3)	3373(7)	0.87
	2326(3)	1253(3)	991(6)	0.69		−868(4)	−623(3)	3354(6)	0.87
	2321(4)	1245(3)	997(7)	1.06		−863(5)	−619(3)	3325(6)	1.10
	2331(4)	1247(3)	997(7)	1.02		−881(4)	−628(3)	3337(6)	0.83
	2352(5)	1237(3)	1017(6)	1.63		−901(5)	−618(3)	3290(7)	1.47
	2377(6)	1259(4)	981(9)	2.08		−928(5)	−600(4)	3275(8)	1.50
D(17)	−2838(5)	1019(3)	−476(7)	0.56	D(20)	443(4)	−1401(3)	3163(7)	0.65
	−2842(5)	1019(3)	−462(7)	0.73		430(5)	−1409(4)	3169(7)	0.71
	−2845(4)	1030(3)	−489(6)	0.98		423(4)	−1396(3)	3144(6)	0.77
	−2839(5)	1002(3)	−487(7)	1.15		432(4)	−1395(3)	3157(6)	0.92
	−2840(5)	1009(3)	−507(7)	1.21		420(4)	−1399(3)	3159(6)	0.98
	−2840(5)	1006(4)	−519(7)	1.62		401(4)	−1403(3)	3150(6)	1.35
	−2779(7)	986(5)	−586(10)	2.43		327(6)	−1398(4)	3119(8)	1.72

Note. Anisotropic B_{ij}'s were refined for all hydrogens (cf. ORTEP plot, Fig. 4), but have been converted in this table to equivalent isotropic B's for conciseness. Note that the B's for the ammonium hydrogens, especially D(13) and D(14), increase to large values near 295 K because of ammonium libration. (The coordinates are listed for each atom in the order of increasing temperature.)

largest amplitudes perpendicular to these bonds as required for librational motion. This is an indication that the relative amplitudes, at least of the anisotropic temperature factors, are physically meaningful; no constraint either explicit or implicit was imposed to fix these ellipsoid axes.

Bond Length Variation with Temperature

Table III lists the bond lengths and angles with their standard deviations for the groups CuO_6, SO_4, ND_4, and three D_2O molecules, plus the hydrogen bonds ND_4—O_4S and $3(OD_2)$—O_4S.

Consider first the water molecules. Since we do not expect any variation of these D—O bond lengths with temperature, we can use these three independent water molecules and seven data sets at different temperatures to see if the calculated standard deviations do represent the observed scatter of the 42 measurements of the D—O distance. Figure 3a shows that for each water molecule, there are no systematic variations with temperature, and that the scatter of points about the mean is indeed represented by the calculated standard deviation. As well, the three independent water molecules have bond lengths all equal within the calculated standard deviations, except perhaps that D(19)—O(9)—D(20) has very slightly longer D—O lengths; this could mean stronger hydrogen bonding of this molecule to the sulfate, since these D(19)—O(5) and D(20)—O(3) are slightly shorter than the other water-sulfate hydrogen bonds. However, the differences appear marginal.

TABLE III

BOND LENGTHS AND ANGLES FOR D-Cu(II) TUTTON'S SALT, WITH Cu(II) AND S VALENCE CHARGES *S* (12)

	Temperature (K)						
	5	50	123	150	203	250	293
Cu(1)–O(7)	2.011(4)	1.996(5)	2.006(4)	2.008(5)	2.024(4)	2.048(5)	2.081(6)
–O(8)	2.304(6)	2.303(6)	2.318(5)	2.318(6)	2.325(6)	2.299(6)	2.242(7)
–O(9)	1.951(4)	1.948(5)	1.950(4)	1.944(5)	1.951(4)	1.941(4)	1.927(6)
–S	2.054(26)	2.098(32)	2.054(24)	2.068(30)	2.006(24)	2.006(26)	2.044(36)
S(2) –O(3)	1.457(8)	1.480(9)	1.469(7)	1.487(8)	1.500(8)	1.446(9)	1.476(12)
–O(4)	1.477(8)	1.491(9)	1.497(7)	1.465(8)	1.481(8)	1.467(9)	1.461(12)
–O(5)	1.504(8)	1.525(8)	1.492(7)	1.514(8)	1.517(8)	1.511(8)	1.488(11)
–O(6)	1.473(9)	1.455(10)	1.460(8)	1.464(9)	1.429(9)	1.469(9)	1.463(13)
–S	6.27 (20)	6.09 (20)	6.24 (20)	6.19 (20)	6.23 (20)	6.37 (20)	6.39 (20)
N(10)–D(11)	1.011(5)	1.006(5)	0.990(4)	0.991(5)	0.994(5)	0.959(6)	0.982(7)
–D(12)	1.047(5)	1.038(6)	1.026(5)	1.043(6)	1.010(6)	0.993(7)	0.946(10)
–D(13)	1.020(6)	1.024(7)	1.014(6)	1.024(7)	1.030(7)	0.963(8)	0.977(11)
–D(14)	1.019(6)	1.018(6)	1.021(5)	1.024(7)	1.018(6)	0.998(7)	0.962(10)
D(11)–O(6)	1.863(5)	1.875(6)	1.885(5)	1.900(6)	1.907(5)	1.968(6)	1.966(8)
D(12)–O(3)	1.902(5)	1.913(6)	1.926(5)	1.914(6)	1.943(5)	2.002(6)	2.094(9)
D(13)–O(4)	1.888(6)	1.856(7)	1.868(6)	1.876(7)	1.892(7)	1.978(8)	2.076(11)
D(14)–O(5)	1.879(6)	1.880(7)	1.880(6)	1.880(6)	1.900(6)	1.920(6)	1.970(10)
O(7) –D(15)	0.980(6)	0.987(7)	0.983(5)	0.983(7)	1.000(6)	0.974(6)	0.978(8)
–D(16)	0.985(17)	0.980(8)	0.983(6)	0.981(7)	0.961(7)	0.979(7)	0.954(10)
O(8) –D(17)	0.991(6)	0.982(6)	0.973(5)	0.969(6)	0.981(6)	0.994(6)	0.999(8)
–D(18)	0.972(7)	0.988(8)	0.964(6)	0.981(7)	0.959(7)	0.969(7)	0.965(9)
O(9) –D(19)	0.994(7)	0.998(7)	0.986(6)	0.992(7)	1.005(7)	0.987(7)	0.991(9)
–D(20)	0.996(7)	0.997(7)	0.999(6)	0.999(7)	1.000(6)	1.023(6)	0.995(8)
D(15)–O(5)	1.767(6)	1.769(6)	1.763(5)	1.767(6)	1.768(6)	1.797(5)	1.809(7)
D(16)–O(6)	1.798(6)	1.795(7)	1.799(6)	1.802(7)	1.797(6)	1.840(7)	1.811(9)
D(17)–O(4)	1.804(5)	1.790(6)	1.792(5)	1.788(5)	1.786(5)	1.773(6)	1.755(7)
D(18)–O(6)	1.877(6)	1.847(6)	1.865(5)	1.863(6)	1.863(6)	1.839(6)	1.824(8)
D(19)–O(5)	1.737(6)	1.725(7)	1.734(6)	1.726(7)	1.712(6)	1.709(7)	1.751(8)
D(20)–O(3)	1.707(6)	1.691(6)	1.711(5)	1.709(6)	1.698(6)	1.700(6)	1.689(8)
O(7) –Cu(1)–O(8)	87.2 (2)	87.9 (2)	87.9 (2)	87.7 (2)	88.1 (2)	87.2 (2)	87.8 (2)
O(8) – –O(9)	88.8 (2)	88.9 (2)	88.5 (2)	88.8 (2)	88.6 (2)	87.9 (2)	88.2 (3)
O(7) – –O(9)	90.2 (2)	90.5 (2)	90.4 (2)	89.9 (2)	90.5 (2)	89.6 (2)	90.5 (3)
O(3) –S2 –O(4)	109.6 (6)	108.1 (6)	108.0 (5)	109.4 (6)	107.8 (6)	110.9 (6)	108.5 (8)
O(3) – –O(5)	108.8 (5)	107.1 (5)	108.6 (4)	106.8 (4)	107.0 (4)	108.9 (5)	108.1 (6)
O(3) – –O(6)	112.6 (5)	113.0 (5)	112.4 (5)	111.6 (5)	111.6 (5)	110.2 (6)	110.0 (7)
O(4) – –O(5)	107.5 (5)	107.2 (5)	106.6 (4)	108.6 (5)	107.3 (5)	108.5 (5)	109.3 (7)
O(4) – –O(6)	108.3 (5)	110.8 (5)	109.4 (4)	111.1 (5)	112.5 (4)	110.7 (5)	111.0 (7)
O(5) – –O(6)	109.9 (6)	110.3 (6)	111.6 (5)	109.2 (6)	110.3 (6)	107.5 (6)	109.9 (8)
D(11)–N(10)–D(12)	111.1 (5)	109.9 (5)	110.7 (4)	109.4 (5)	113.4 (5)	109.2 (6)	109.0 (8)
D(11)– –D(13)	112.0 (5)	112.5 (6)	114.1 (5)	112.6 (6)	115.0 (5)	114.0 (6)	111.0 (8)
D(11)– –D(14)	108.4 (5)	109.0 (5)	108.9 (4)	109.8 (5)	108.4 (5)	108.9 (6)	104.1 (8)
D(12)– –D(13)	108.5 (5)	108.8 (5)	108.2 (4)	107.7 (5)	107.7 (5)	109.2 (6)	113.2 (9)
D(12)– –D(14)	108.1 (5)	107.7 (5)	106.1 (4)	107.8 (5)	105.9 (5)	106.2 (6)	106.6 (9)
D(13)– –D(14)	108.7 (5)	108.8 (5)	108.6 (4)	109.5 (5)	105.9 (5)	109.1 (6)	112.4 (10)
D(15)–O(7) –D(16)	106.6 (5)	106.0 (6)	107.1 (5)	106.3 (5)	108.5 (5)	104.9 (5)	107.2 (7)
D(17)–O(8) –D(18)	104.8 (5)	104.8 (6)	105.9 (5)	107.9 (6)	107.4 (6)	105.3 (6)	103.8 (7)
D(19)–O(9) –D(20)	107.8 (6)	106.1 (6)	106.9 (5)	106.2 (6)	105.3 (6)	104.8 (6)	103.5 (8)

Note. The order of the bonds is Cu—OD_2, S—O_4, N—D_4, ND_4—O_4S hydrogen bonds, 3 O—D_2 and OD_2—O(4)S hydrogen bonds. The valence charges were calculated from the bond lengths using the Brown–Shannon constants (1.718, 6.0) for Cu(II) and (1.629, 4.6) for S (15).

For the sulfate group (Fig. 3b), we have 28 measurements of the S—O distance. Again, there is no obvious systematic variation with temperature, except perhaps a slight apparent shortening at higher temperatures: this might indicate libration of the sulfate group, which would produce an apparent shortening of the distance between S and the mean center of mass of oxygen. Our isotropic oxygen vibration amplitudes

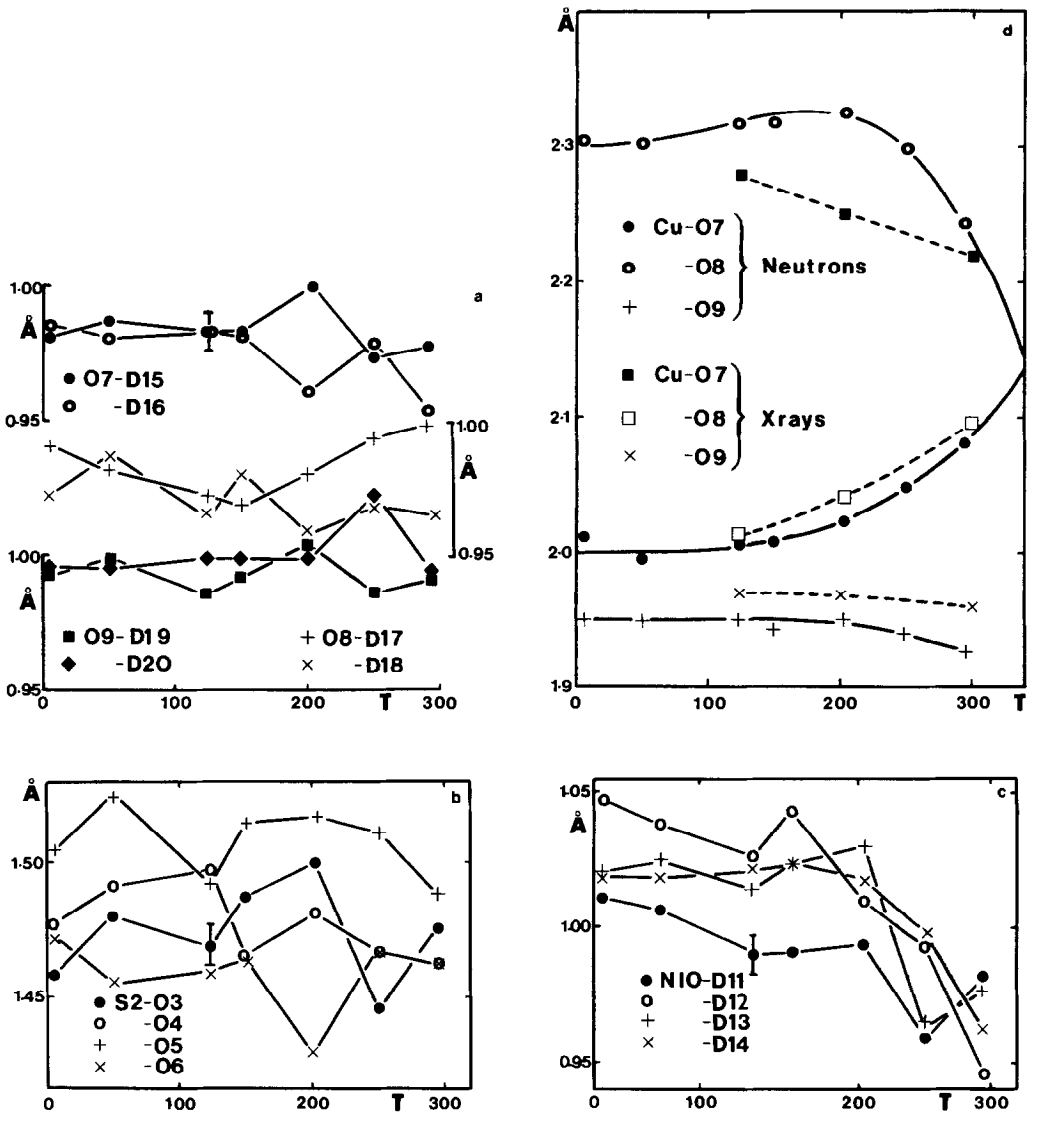

FIG. 3. (a) The O—D_2 water bond lengths in Cu(II) Tutton's salt are virtually all equal and constant with temperature between 5 and 295 K. (b) The sulfate bond lengths are again almost all equal and independent of temperature. Very small systematic differences are probably due to different hydrogen bond strengths for different oxygens. (c) The N—D_4 ammonium bond lengths are almost all equal, but apparently decrease with temperature. This decrease is a familiar artifact; the strong libration of this ion is not exactly modeled by simple anisotropic temperature factors for the hydrogens. (d) The Cu—OD_2 bonds are the only ones which really change with temperature. The usual elongated CuO_6 octahedron is only slightly distorted near absolute zero, but as the temperature is increased, Cu—O bonds near the *xy* plane become more nearly equal. The compressed CuO_6 octahedral configuration is approached, with a structural transition predicted near 340 K. Note that Cu—O7 is the long bond for the hydrogenous compound (X rays), while Cu—O8 is the long bond for the deuterated material (Neutrons).

do not of course model any such libration; this may also be the reason why the scatter in S—O bond lengths is about 1.5 times the calculated standard deviation. Again, there are small systematic differences between the different S—O bonds, due presumably to some sulfate oxygens being more strongly hydrogen bonded than others: for example, each oxygen has one hydrogen bond with an ammonium deuterium, and one with a water deuterium, except O(5) and O(6), which are bonded to two water molecules as well as to ammonium.

The N—D bond lengths obtained for ammonium (Fig. 3c) show a much more obvious decrease with increasing temperature. This artifact is due to the strong libration of the ammonium ion; the deuterium ion distribution is then banana shaped rather than ellipsoidal as in our anisotropic deuterium model, and the center of density of this banana-shaped distribution is displaced toward the center of libration, the nitrogen atom. Correction of the N—D bond lengths for this effect (*12*) would eliminate this systematic reduction. Apart from this, the scatter of the N—D bond lengths again appears to be consistent with the calculated standard deviations: N(10)—D(11) is slightly smaller, presumably due to hydrogen bonding, but the difference disappears at higher temperatures when libration reduces such bonding effects.

The Cu—O bond lengths (Fig. 3d) behave quite differently. First, Cu—O(8) is very much longer than Cu—O(7), which is itself somewhat longer than Cu—O(9). This pattern is the same as that observed in the isomorphous alkali Tutton salts, but different to that found in the hydrogenous ammonium salt (*5, 10, 11*), where Cu—O(7) is longer than Cu—O(8). A check was made for a false minimum by restarting the refinement with the X-ray coordinates (Cu—O(7) long), but the initial fit was poor, and the structure immediately refined back to the (Cu—O(8) long) result. It is this rhombic distortion of the CuO_6 chromophore (1) that we wish to understand.

Second, Cu—O(8) decreases smoothly with increasing temperature, Cu—O(7) increases smoothly, and Cu—O(9) remains almost constant, falling only slightly. Instead of one long and two short bonds at low temperature, at ambient temperature we have one long, one short, and one medium Cu—O bond. This temperature-dependent effect was also indicated by the earlier X-ray results on the hydrogenous material (*3, 5*); the present experiment extends that work to near absolute zero, and includes many more temperature points.

Finally, for each Cu—O bond, and within the calculated standard deviations, the points appear to lie on smooth curves as a function of temperature: these effects are much larger than the experimental errors. It remains to explain why the Cu—O bond lengths behave differently to the N—D, S—O, and D—O distances as a function of temperature.

It is important to notice that the lattice constants vary remarkably with temperature (Fig. 2). The *c* axis increases rapidly near 295 K, while *a*, *b*, and the angle decrease rapidly. This behavior is typical of a second-order phase transition somewhat above room temperature. Such a phase transition may be due to the onset of (hindered) rotation of the ammonium ion. The four ammonium ion tetrahedra in the cell have apexes pointing approximately along *c*; two pointing up and two pointing down (Fig. 4). For any one tetrahedra, the difference in lattice energy between pointing up and pointing down is probably very small; the transition could therefore involve flipping of the ammonium tetrahedra between the two configurations. This would force an expansion of the structure along *c*, and allow contraction in the other directions, as observed.

This strong expansion along *c* does not seriously change the Cu—O(9) bond dis-

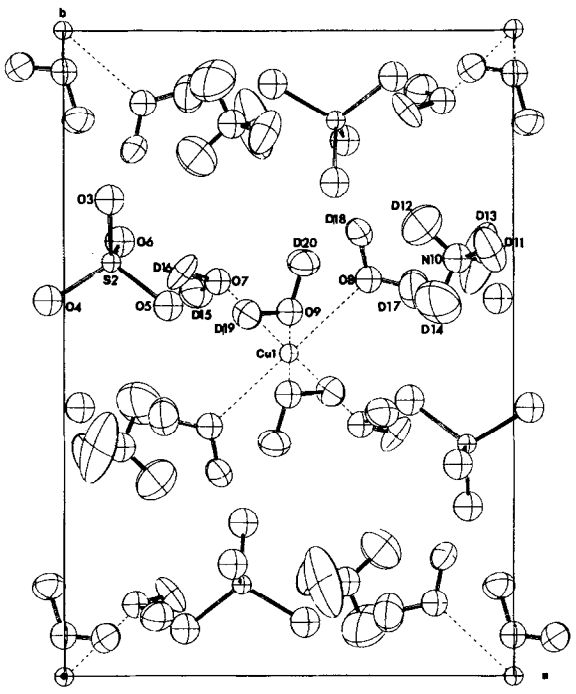

FIG. 4. ORTEP projection of the structure down the c axis. Notice the four ND_4 tetrahedra, two pointing down the c axis, labeled N10-D13, and two pointing up. Flipping of these tetrahedra are apparently responsible for the predicted phase transition near 340 K.

tance, which is directed mainly along this axis: these water molecules are most strongly bound to copper, the Cu—O distance being the shortest. However, expansion along c does allow space for the remaining two pairs of water molecules to become more nearly equivalent. The usual elongated octahedral (4 short-2 long) Cu—O bonding, which is seen at low temperatures, changes at high temperatures to the compressed octahedral (2 short-4 long) bonding. By extrapolation of the Cu—O bond lengths in Fig. 3d, the transition should occur at about 340 K.

With X rays, we would not have noticed the onset of hindered rotation of the $(NH_4)^+$ groups, since the hydrogen atoms would have been barely visible. We might then have attributed such a phase transition to a simple order–disorder of the Jahn–Teller elongated axis between the two bonds near the x-y plane, such as in $A_2PbCu(NO_2)_6$ where A = K, Rb, Cs (*13*). This would not, though, explain the rapid increase in the length of the c axis. In Cu(II) Tutton's salt, it seems that $(ND_4)^+$ rotation may be the driving force allowing the long Cu(II)—O axis to become equivalent to one of the shorter axes. This might then permit a dynamic Jahn–Teller switching as a consequence, rather than a cause of the transition. Then even in a structure as simple as this, we should not interpret changes in the Cu(II) coordination simply in terms of the local environment, neglecting the influence of the remainder of the structure.

The X-ray Cu—O results, also shown on Fig. 3d, follow a similar trend, indicating a transition above room temperature. The fact that the roles of the almost structurally equivalent O(7) and O(8) oxygens are interchanged in the hydrogenous salt is further

evidence that the octahedral distortions from tetrahedral symmetry are due less to Cu—O bonding forces than to the environment, and in particular, to the hydrogen bonding of the $Cu(OH_2)_6^{2+}$ complex.

An interesting check on the reliability of the Cu—O bonds is obtained by calculating the sum of the bond strengths and hence the copper valence bond charge according to Brown and Shannon (*14*, *15*). The valence charge S at each temperature (Table III) is given by

$$S = \sum_{iS_i} = \sum_i \frac{R_{Cu-Oi}^{-N_{Cu-O}}}{R_{Cu-O}}$$

where $R_{Cu-O} = 1.718$ and $N_{Cu-O} = 6.0$ for Cu(II) according to the latter authors. The summation is over the six bond lengths R_{Cu-Oi}. The result is clearly independent of temperature, with a normal scatter about a mean Cu(II) valence charge of 2.05 ± 0.03, not significantly different from 2. This in spite of the very different Cu—O*i* bond lengths or bond strengths s_i. The formal valence charge on sulfur is slightly higher than the expected 6, but similar values are obtained with the X-ray results; this is presumably due to slightly inappropriate Brown–Shannon parameters rather than to any real charge transfer to sulfate.

Conclusion

Using neutron powder diffraction, we have plotted the structure and bonding in deuterated Cu(II) Tutton's salt at many more temperature points than is usual with single-crystal methods. This allows an appreciation of the evolution of structural parameters with temperature, and the study of this evolution proved to be the key to understanding the structure. Apparently there is a smooth transition between a completely ordered structure with elongated octahedral Cu(II)—O bonding at low temperature, to a structure in which $(ND_4)^+$ rotation stretches the *c* axis, permitting the long and the short Cu(II)—O bonds in the *xy* plane to become more nearly equivalent, and both longer than the remaining short bond along *c*, i.e., compressed CuO_6 octahedral bonding.

This may be only a pseudo compression due to dynamic disorder of the Jahn–Teller elongated Cu(II)—O axis between the two bonds near the *xy* plane, but this experiment provides no evidence to support that hypothesis since the Cu(II) and water O vibrational amplitudes are not unusually large. In any case, the explanation of changes in Cu(II) coordination cannot be limited simply to the local environment of this atom, but must also take account of the changing packing requirements of the remainder of the structure, and in particular the hydrogen bonding of the $(ND_4)^+$ ions. The importance of hydrogen bonding in changing the balance of forces is emphasized by the fact that Cu—O(8) is the long bond in the deuterated material, as in the alkali salts, while the almost equivalent Cu—O(7) bond assumes this role in the hydrogenous ammonium salt.

Neutron powder diffraction was essential for this study; it permitted many temperatures, from near absolute zero up, to be examined rapidly, and it revealed the strong libration of the $(ND_4)^+$ ion, the hydrogens of which would have been barely visible with X rays.

References

1. A. F. WELLS, "Structural Inorganic Chemistry," Oxford Univ. Press (Clarendon), London/New York (1975).
2. B. J. HATHAWAY AND D. E. BILLING, *Coord. Chem. Rev.* **11**, 143(1970); A. MURPHY, J. MULLANE, AND B. HATHAWAY, *Inorg. Nucl. Chem. Lett.* **16**, 129 (1980).
3. M. DUGGAN, A. MURPHY, AND B. J. HATHAWAY, *Inorg. Nucl. Chem. Lett.* **15**, 103 (1979).
4. B. J. HATHAWAY, M. DUGGAN, A. MURPHY, J. MULLANE, C. POWER, A. WALSH, AND B. WALSH, *Coord. Chem. Rev.* **36**, 267 (1981).

5. N. W. ALCOCK, M. DUGGAN, A. MURPHY, S. TYAGI, B. J. HATHAWAY, AND A. W. HEWAT, *J.C.S. Dalton Trans.*, in press (1984).
6. A. W. HEWAT AND I. BAILEY, *Nucl. Instrum. Methods* **137,** 463 (1976).
7. A. W. HEWAT, "POWDER, A Computer Program System for Neutron Powder Diffraction," ILL Internal Report (1977).
8. H. M. RIETVELD, *J. Appl. Crystallogr.* **2,** 65 (1969).
9. A. W. HEWAT, "The Rietveld Program for the Profile Refinement of Atomic and Magnetic Structures—Modified for Anisotropic Thermal Vibration," Harwell Report 73/239 and ILL Report 74/H62S (1973).
10. H. MONTGOMERY AND E. C. LINGAFELTER, *Acta Crystallogr.* **20,** 659 (1966).
11. G. M. BROWN AND R. CHIDAMBARAM, *Acta Crystallogr. B* **25,** 676 (1969).
12. W. R. BUSING AND H. A. LEVY, *Acta Crystallogr.* **17,** 142 (1964).
13. H. G. VON SCHNERING, *Z. Anorg. Allg. Chem.* **400,** 200 (1973).
14. I. D. BROWN AND R. D. SHANNON, *Acta Crystallogr. A* **29,** 266 (1973).
15. I. D. BROWN AND K. K. WU, *Acta Crystallogr. B* **32,** 1957 (1976).